Variability caused by Setup and Operating Conditions for Conducted EMI of Switched Mode Power Supplies over the 2-1000 kHz Interval

Variability caused by Setup and Operating Conditions for Conducted EMI of Switched Mode Power Supplies over the 2-1000 kHz Interval

Andrea Mariscotti, *Senior Member, IEEE,* Leonardo Sandrolini, *Senior Member, IEEE,* and Gaetano Pasini

***Abstract*—The measurement of conducted emissions of Switched Mode Power Supplies (SMPSs) is discussed for the 2-1000 kHz frequency range, analyzing variability caused by setup elements and test conditions. The tested SMPSs have 12 VDC output and about 20 W nominal power. They are fed by a controlled AC power supply, instead of mains, through a Line Impedance Stabilization Network and various loading levels are applied. Identified causes of variability (supply voltage and frequency variations, thermal stabilization influencing internal mechanisms of emissions) indicate a relevant impact on the spread of measured conducted emissions, ranging from a fraction of dB to about 10 dB (sample standard deviation). Such phenomena represent a cause first of all of systematic error, but also of increased uncertainty. No EMC standards are known to take them into account, nor the scientific literature reports extensive quantification, as in the present case. The shift of the line spectrum of emission consequential to a mains frequency change revealed to be exploitable also for better identification of internal sources of emission.**

***Index Terms*—AC-DC power converters, Conducted emissions, Electromagnetic interference, Supraharmonics, Test conditions, Variability, Uncertainty.**

I. Introduction

MODERN electronic products (information technology, audio, video and entertainment, and mobiles, to exemplify the most widespread) are supplied and interfaced with the Low Voltage mains using Switched-Mode Power Supplies (SMPSs). Fundamentally based on an input rectifier and a switching step-down converter, they provide a DC output of 5 to 24 V with power of some to tens of Watts. Such a low power rating provides a waiver for the application of harmonic limits to the input AC current [1], as well as suggests a lesser role as source of higher-frequency emissions. On the contrary, limits of emissions are identical to other electronic equipment and larger converters (all disciplined by EMC standards such as EN 55011 [2] and EN 55032 [3]). In addition, SMPSs are deployed in residential and office environments in a large number, becoming a relevant EMI source in terms of spectrum occupation and amount of emissions per W of installed power. Conducted emissions in fact feature switching components, ringing and impulsive terms polluting a wide frequency interval, including the frequency range recently identified with the term "supraharmonics". For this standardization is lagging to identify suitable limits and measurement techniques to fill the gap between harmonics (up to 2 kHz) and RF conducted emissions (starting at 150 kHz).

The reasons to focus on the supraharmonic 2–150 kHz interval are the significant propagation and penetration, the relatively large intensity possibly exciting network resonances, besides causing problems of interference, aging and heating [4]. This frequency interval has been indeed included in some standards [5]–[7] that, however, do not cover SMPSs. SMPSs and switching converters may exacerbate network resonances and disturbance propagation if the effect of the front-end filters is considered [8], as well as some degree of differential- to common-mode conversion due to the variation of the geometrical imbalance in the circuit.

Emissions of this kind should be processed with methods closer to the RF interval rather than harmonics, and this is why a 2 kHz aggregation bandwidth is proposed in the IEC 61000-4-30 [9], broader than the 200 Hz of the IEC 61000-4-7 [10] and closer to the 9 kHz resolution bandwidth (RBW) used for RF interval [11]. Selecting the right RBW is a compromise between accurate amplitude estimate of spectral components and adequate tracking of impulsive parts. RBW in fact not only affects the general shape of the spectrum (e.g. separability of adjacent components and displayed noise floor), but also the amplitude estimate, as considered in [12]. In a time-domain approach, the RBW is basically related to the duration of the transformation window, to adapt to the duration of the switching byproducts and disturbance repetition rate [13].

Besides instrumentation uncertainty, there are other sources of uncertainty related to the setup and the operation of the SMPS under test (from now on EUT, equipment under test). Whereas the former is well documented in instrumentation manuals and datasheets and is subject to periodic verification and quantification (calibration), the latter is often overlooked for several reasons: its quantification is more complex (amount of repeated tests), it necessitates a more refined statistical analysis, and it is often deemed under control by following general EMC good practice and standards indications. This would be correct if EMC product standards go into the details of the EUT operation. Basic EMC standards, instead, cover instrumentation and settings, horizontally covering different, but similar, types of emission measurements, but do not delve into the behavior and characteristics of EUTs.

A. Mariscotti is with the Department of Electrical, Electronic and Telecommunications Engineering and Maritime Architecture, University of Genova, I-16145 Genova, Italy (e-mail: andrea.mariscotti@unige.it).

L. Sandrolini and G. Pasini are with the Department of Electrical, Electronic, and Information Engineering "Guglielmo Marconi," University of Bologna, I-40136 Bologna, Italy (e-mail: leonardo.sandrolini@unibo.it; gaetano.pasini@unibo.it).

For conducted emissions, excluding external sources in the same frequency range as decoupled at a large extent by the use of LISN (Line Impedance Stabilization Network), relevant causes of variability are supply conditions and stabilization of the thermal regime, especially for the influence on internal mechanisms of emissions that are scarcely known and possibly variable between types and architectures. This was preliminarily shown in [12], of which this work is an extension in terms of better quantification with more experimental data and inclusion of new sources of variability. Quantifying variability and its causes, thus fostering repeatability and reproducibility, is particularly important considering the many works evaluating and analyzing SMPS emissions [14], [15].

Following these considerations, the paper is structured discussing in Section II typical SMPS emissions and measurement setup. Then, Section III provides details of the causes of variability other than the instrumental one, related, as said, to supply and operating conditions. Such analysis is then supported by a wide set of measurement results in Section IV, taken in both time and frequency domains, using a purposely developed Labview automated setup. Section IV is completed by a discussion of results, providing input to EMC standards to ensure stable operating conditions and quantification of variability of measured data. Section V presents conclusions and indications for further activity.

II. Emission mechanisms and measurement setup

A. SMPS operation and emission mechanisms

SMPSs in their simplest implementation contain an input bridge rectifier feeding some form of switching converter, such as a buck (step down) converter for cheapest implementations, or a half or full H-bridge for higher power ratings. Often SMPSs are synchronized to the mains frequency, so to achieve various objectives: minimization of losses and voltage stress on components, increasing expected life at the same time and achieving power factor control operation, PFC (whether implemented in a separate buck stage or integrated in the rectifier as a bridge-less PFC). SMPS conducted emissions contain the switching fundamental, its harmonics, and other high-frequency narrowband components (such as caused by ringing), together with non-stationary low-frequency components caused by the main pulses, superposed to the mains fundamental [16]. Such mixed components feature different bandwidth, level of stationarity and in general time dependency. Measurement results depend on instrumentation settings and parameters, whose effects are well documented and to some extent can be compensated for to compare different measurements. This leads to prefer time-domain (TD) measurements for the flexibility in post-processing.

The studied SMPSs have emissions waveforms (signal y_1 in Fig. 2) characterized by impulses repeating every 10 ms (see Fig. 1). The 10 ms timebase is of course provided by the ripple of single-phase rectification of the 50 Hz mains voltage (the repetition interval reduces to 8.33 ms for a 60 Hz mains fundamental). Each impulse is followed by various oscillatory terms and an anti-symmetrical duality can be caught for pairs of adjacent impulsive bursts.

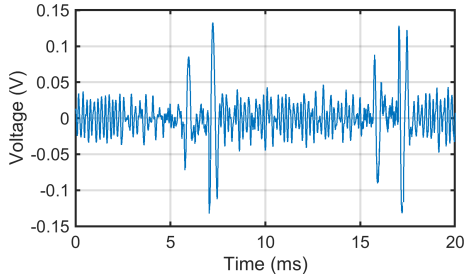

Fig. 1: Time-domain waveform of the high-pass filtered LISN output y_1 for LaCie P90 power level after thermal stabilization.

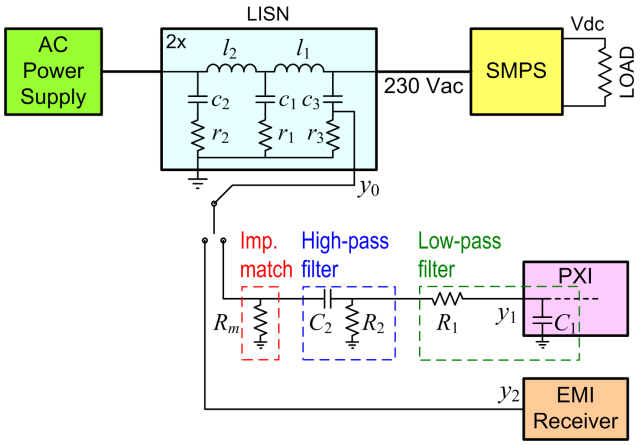

Fig. 2: Scheme of the experimental setup: SMPS under test and its configurable load fed by the DC output; LISN (scheme from [18] for one phase with l_1=50 µH, l_2=250 µH, r_1=5 Ω, c_1=8 µF, r_2=10 Ω, c_2=4 µF, r_3=1 kΩ, c_3=0.25 µF); 50 Ω impedance matching resistor R_m; high-pass filter C_2R_2; low-pass filter R_1C_1 (exploiting internal PXI input capacitance); PXI acquisition system; EMI Receiver.

The swept spectrum of emissions for a repetitive pulsed signal is a line spectrum: the repetition rate (nominally 100 Hz) gives line separation, with amplitude determined by the envelope of the spectra of observed pulses and oscillations. For a change of mains frequency e.g. due to instability, there will be an amplified shift of the bins (proportional to the harmonic order) and a slight variation of the height of the intercepts of the envelope spectrum and of the displayed amplitude, as discussed in sec. III.B.

B. SMPSs characteristics and test setup

The tested SMPSs are supplied at 230 V AC mains voltage by a controlled power supply (CPS) HP6834B [17] through the LISN, which provides a reading of the unsymmetrical voltage on each phase, decouples the mains upstream filtering off disturbance, and guarantees a normalized impedance for reproducibility. The experimental setup is shown in Fig. 2.

SMPSs are connected to a configurable resistive load to test in particular two power levels, 25% and 90% of the nominal power, noted as P25 and P90. The tested SMPSs are:

- LaCie 12 Vdc output, 26 W nominal power, fixed frequency modulation (identified as “LaCie”);
- Shenzhen Honor Electronics, 12 Vdc output, 18 W nominal power, random modulation (identified as “Shenzhen”);

The load is made of a configurable set of $10\,\Omega$ Alu housed power resistors with 5% tolerance and $50\,\mathrm{W}$ rated power, mounted on an Alu heatsink with thermal grease. The resistors have anti-inductive construction and a low thermal coefficient of only $50\,\mathrm{ppm/°C}$. P25 and P90 conditions are achieved with some approximation by configuring as follows: for the LaCie $25\,\Omega$ and $6.67\,\Omega$, corresponding to 23.8% and 88.6% loading; for the Shenzhen $33.3\,\Omega$ and $8.33\,\Omega$ corresponding to 25.6% and 90.3% loading. Correct loading was verified by means of voltage and current readings on the output circuit (carried out with Fluke multimeter mod. 177 with ±0.2% and ±1.0% of accuracy for DC voltage and current measurements, respectively). At different loading levels the DC output voltage varies starting from a no-load value that is already quite different from the nominal $12\,\mathrm{V}$, so that the load value was adapted with some trial and error to meet the P25 and P90 conditions with a ±1.5% maximum error.

Emissions are sampled in time domain with a 14-bit PXI system (model 5164) sampling at $10\,\mathrm{MSa/s}$ and replacing the 8-bit digital sampling oscilloscope used in [12]. Anti-aliasing low-pass RC filter is provided with a corner frequency of $2\,\mathrm{MHz}$, selecting series resistor R_1= $3.9\,\mathrm{k\Omega}$ tuned to the input capacitance C_1 of the PXI system, approximately $20\,\mathrm{pF}$. R_1 is responsible for a slight attenuation of the signal amplitude (systematic error), in the order of 0.4% (the ratio of the so created voltage divider with the $1\,\mathrm{M\Omega}$ input impedance of the PXI board).

The LISN transfer function is such that attenuation of network distortion is provided only for a frequency interval compatible with the target measurement, the RF conducted emissions above $9\,\mathrm{kHz}$.Such attenuation is identified in CISPR 16-1-2 [18] as decoupling factor (DF) or isolation. An estimate of DF variation with frequency is provided in [19], showing a reduction down to a minimum of $24\,\mathrm{dB}$ at about $7.5\,\mathrm{kHz}$, yet higher than the minimum requirement of $0\,\mathrm{dB}$ at $9\,\mathrm{kHz}$ [18]. The CPS ensures low and repeatable distortion, limited to 1% up to $1\,\mathrm{kHz}$ [17]; to further attenuate leakage of grid distortion into the acquired signal, a high-pass filter on the y_1 signal line is advisable.

For differential measurements the setup should be different, to avoid out-of-scale and saturation, in case the minimum frequency of interest remains 2 kHz [20].

The high-pass filter cutoff frequency is set for this work to $1\,\mathrm{kHz}$ (i.e. one octave below the minimum frequency of $2\,\mathrm{kHz}$). The setup of [12] proposed $1.5\,\mathrm{k\Omega}$ and $100\,\mathrm{nF}$, as a compromise not to impact on the $50\,\Omega$ source impedance and for the availability of capacitors with good high-frequency performance: the signal source impedance may be assumed $50\,\Omega$ in case of LISN (obvious), but also for voltage or current readings in general, as high-frequency probes are usually impedance matched to $50\,\Omega$. The use of a high-pass filter is in agreement with [20] and follows also the recommendation of the IEC 61000-4-30 [9].

For frequency domain measurements an EMI receiver was used, set to Peak detector and with RBW values selected for the specific test: fine step ($2.5\,\mathrm{Hz}$) and small RBW ($10\,\mathrm{Hz}$) for the spectrum lines shift test, otherwise $1\,\mathrm{kHz}$ to adequately follow the impulsive part of the signal [12].

The setup is controlled through the PXI board with custom-made code, that manages time-domain acquisitions, settings and sweeps of the EMI receiver, timing of acquisitions (especially for long-term recordings), preview and data storage.

III. Sources of variability

Variability of the mechanisms of emissions, of the test and environmental conditions, and their impact on the final uncertainty of spectrum amplitude are presented and discussed in the following and demonstrated experimentally in Section IV.

A. Foreword on instrumental uncertainty

Instrumental uncertainty is in general considered as the only relevant element to determine the uncertainty of measurement results: it is well defined and lends itself to a Type B approach, based on the information provided by manufacturers and CISPR 16 standards [11], [18]. CISPR 16 discusses characteristics and uncertainty of RF instrumentation, as a guideline for purchase and use, focusing on an extended frequency range that only partially covers the present problem.

The instrumental uncertainty of the most relevant items of equipment can be summarized as follows:

- The Rohde & Schwarz EMI Receiver mod. ESRP 7 GHz has a total amplitude uncertainty of $0.47\,\mathrm{dB}$ at k=2 coverage factor [21].
- The National Instrument PXI board mod. 5164 [22] is a 14-bit $1\,\mathrm{GSa/s}$ acquisition system, with an amplitude uncertainty of $\pm 0.1\,\mathrm{dB}$ ($k = 2$) for full-scale signals ($\pm 1.15\,\mathrm{dB}$ for signals $\leq$ 1% full scale), frequency response flatness of $\pm 0.05\,\mathrm{dB}$, THD of $-73\,\mathrm{dBc}$ and total rms noise of 0.07% for the $250\,\mathrm{mVpp}$ scale.
- The LISN ESH2-Z5 $9\,\mathrm{kHz}$–$30\,\mathrm{MHz}$ is declared compliant [23] to CISPR 16-1-2 [18], so with a maximum deviation of ±20% with respect to the nominal impedance curve over the $9\,\mathrm{kHz}$ to $30\,\mathrm{MHz}$ interval. However, at the lower end of the nominal frequency range, the influence of the power grid impedance upstream may be relevant, as pointed out in [19], where the observed variability of LISN impedance is $1.5\,\mathrm{dB}$ at $9\,\mathrm{kHz}$, $2.8\,\mathrm{dB}$ at $4\,\mathrm{kHz}$ and $5\,\mathrm{dB}$ at $2\,\mathrm{kHz}$.
- Each LISN has a voltage division factor (VDF) that describes the attenuation of the measured signal introduced by the less-than-ideal response, in particular at low frequency. The VDF is compensated by the measured correction factor (CF) that represents the LISN calibration (carried out with a spectrum analyzer with tracking generator). The CF of the used LISN is shown in Fig. 3 and the residual uncertainty is $\pm 0.6\,\mathrm{dB}$ ($k = 2$).
- The HP6834B controlled power supply is a relevant element for the uncertainty of the supply voltage and frequency: as per datasheet such uncertainties are 0.15% + $0.3\,\mathrm{V}$ between 45 and 100 Hz, and 0.01% + $10\,\mu\mathrm{Hz}$, respectively.
- Temperatures have been measured with Pt100 sensors applied to the SMPS top and bottom surface, avoiding air flow to cause temperature gradients. The accuracy over

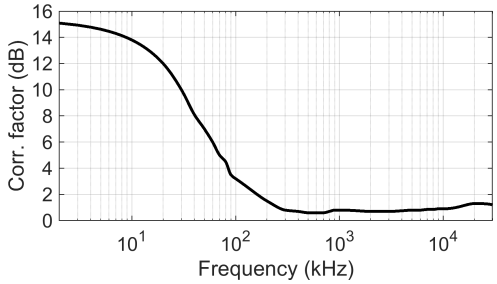

Fig. 3: LISN ESH2-Z5 correction factor.

the 0–400 °C interval is ±0.1 % ±0.6 °C, thus amounting to $<$ ±0.65 °C for the observed maximum temperature excursion between 20 °C and 50 °C.

Considering the peculiar characteristics of SMPS emissions (mixed broadband impulsive components and narrowband components, with some degree of non-stationarity), time-domain measurements have allowed adapting settings to the specific necessity of the analysis. The reference for uncertainty and systematic errors introduced with the Short-Time Fourier Transform (STFT) was analyzed in [13]. Conversely, for frequency-domain measurements the effect of RBW on spectrum amplitude for steady and transient phenomena was considered in [12], [24].

B. Effects of supply and operating conditions

Supply voltage conditions are relevant to uncertainty, but their effect depends on the EUT characteristics, never considered in EMC normative procedures. For a certain class of EUTs (such as LED and fluorescent lamps [25]–[27]) a significant sensitivity of emissions to supply voltage changes reflects then in an increased uncertainty and issues of repeatability. The following points then should be taken into account.

- Mains voltage and output voltage level: first, a change in the latter due to a variation of the former may affect emissions (line regulation capability); second, the direct influence of the mains voltage was evaluated in [27] and found not always negligible.
- Mains frequency change does not impact directly on EUT emissions. What is affected is the positioning on the frequency axis of the bins of the line spectrum, that are directly determined by the input rectifier ripple; this in turn affects the intercept of the underlying continuous spectrum and the resulting amplitude of each line that can be measured. A model is provided below.

A static scenario is considered where the experiment is carried out with two different mains frequency values, f_{m1} and $f_{m2} = f_{m1} + \Delta f$, with resulting rectifier ripple $2f_{m1}$ and $2f_{m2}$, which determines the spacing of the line spectrum bins. With a simplified approach, two types of waveshapes are assumed for the EUT emission: a rectangular pulse $r(t)$ (simulating semiconductor switching) and a P-period oscillation (simulating the consequential ringing).

The continuous spectrum $R(f)$ of $r(t)$ is the well-known normalized sinc function, with the first zero at $1/\tau$, τ being the pulse width (or duration). The P-period oscillation, being the product of the rectangular pulse with a sinusoidal signal (the oscillation) at an arbitrary frequency f_o, will result in $R(f)$ moved at the frequency f_o, with the pulse duration τ equal to P periods, namely P/f_o. If we assume that a bin of the line spectrum coincides with the tip of $R(f - f_o)$ for the mains frequency f_{m1} (that is equivalent to say that f_o is an integer multiple N_{fo} of f_{m1}), then the resulting change of height of the intercept of the line spectrum when the mains frequency is f_{m2} will be $\mathrm{sinc}(\pi N_{fo}\Delta f/P)$.

Assuming small Δf, the effect on the line spectrum will be that of a shift of the lines, keeping the initial harmonic order (no "hopping" of lines, as $N_{fo}\Delta f < 2f_{m1}$). For a small shift the sinc function can be approximated by its first non-null Taylor series term, i.e. the 2nd order term $-x^2/6$, where x is the argument of the sinc centered on f_o. The height reduction ΔA (the maximum reduction for the largest and most significant components of a group) will then be

$$\Delta A = -(\pi N_{fo}\Delta f/P)^2/6 \tag{1}$$

Similarly to supply conditions, selected EUT operating points for testing should be representative for what regards emissions. Three factors in particular should be considered:

- Relevance of selected operating points: the "no load" condition is known to cause particularly large emissions in some cases; then, as SMPSs are designed for energy efficiency, it is almost likely that at some intermediate load level the controller changes between various modulation patterns, such as pulse skipping, reduction/increase of base frequency, random/fixed modulation.
- Load stability and RF characteristics: heating of load components must be controlled at best to avoid large resistance variations (e.g. Alu housed resistors may have thermal coefficients in excess of $300\,\mathrm{ppm/°C}$); the load should be as linear as possible and void of parasitics, in particular capacitance to ground, as instead may happen with electronic loads.
- EUT thermal behavior and influence on intensity and distribution of emission components: EUT self-heating is unavoidable and thermal transients occur when new load conditions are applied; the effects on emissions are various, as internal temperature affects semiconductors and capacitors, in particular. It is not known of EMC standards indicating a minimum time interval for stabilization or how to check it: this is evaluated experimentally in Section IV.

C. Short- and long-term variability

Variability is evaluated in the following in terms of classical and robust statistics: mean μ, median m, dispersion σ and inter-quartile range q. The name "indexes of dispersion" is used then to identify the ratios σ/μ and q/m. The reason for using robust statistics is that spectra of emissions are in general characterized by outliers. This is demonstrated by the significant distance of max hold profile from the mean and median profiles. A robust statistic is the use of quasi-peak detection, that "forgets" large peak values occurring seldom, compared to its time constant [11]. The use of max

hold or quasi-peak bring to irreversible measurements and do not allow a confidence interval to be estimated. Frequency intervals with low dispersion are identified and considered in particular as an indication of coherent emissions related to stable mechanisms of emissions, once a satisfactory thermal equilibrium has been reached.

Time axes j and k are considered for short- and long-term variability. STFT is calculated over time windows of duration $T = 10\,\mathrm{ms}$, to bracket at least one emission interval, splitting records of duration $T_{rec} = 3\,\mathrm{s}$ into $J = T_{rec}/T = 300$ non-overlapped windows (along time axis j). The time axis k has a coarser time step $\Delta T_{rec} = 10\,\mathrm{min}$ and is used for EUT thermal transient. The overall set of spectra is arranged in the 3-D matrix $S(i, j, k)$.

Statistical quantities are thus referred to as short or long range using "st" and "lt" subscripts over indexes j and k.

$$\mu_{st}(i,k) = \frac{1}{J}\sum_{j=1}^{J} S(i,j,k) \tag{2}$$

$$\mu_{lt}(k) = \frac{1}{I}\sum_{i=1}^{I} \mu_{st}(i,k) \tag{3}$$

$$\sigma^2_{st}(i,k) = \frac{1}{J}\sum_{j=1}^{J} (S(i,j,k) - \mu_{st}(i,k))^2 \tag{4}$$

$$\sigma^2_{lt}(k) = \frac{1}{I}\sum_{i=1}^{I} (\mu_{st}(i,k) - \mu_{lt}(k))^2 \tag{5}$$

Robust statistics can be easily implemented by using the equations above, where mean and dispersion are replaced by median m and inter-quartile range q.

IV. Results

The scenarios and parameters introduced in Section III are here evaluated with the help of experimental results, either captured in frequency or time domain.

A. Line spectrum and frequency stability

Tests were done using the 230 V power supply, setting a deviation from the 50 Hz of ±10 mHz and observing the resulting frequency shift and amplitude change of the most relevant narrowband components (shown in Fig. 4). The accurate amplitude estimate of selected components under a fundamental frequency shift is hindered, first, by the normal amplitude fluctuation due to short-term instability of operating conditions (as such measurements with fundamental frequency shift are taken at different times, although in close succession) and, second, by the instrumentation amplitude uncertainty.

The observed amplitude change goes from very small variations of both signs to the most significant reductions of amplitude up to 0.12 dB. Eq. (1) for the present case, assuming a long duration of oscillations as visible in Fig. 1 and thus a P value in the order of a hundred (taken equal to 100), gives exactly 0.125 dB, confirming this order of magnitude for a change of amplitude due to a ±10 mHz mains frequency shift.

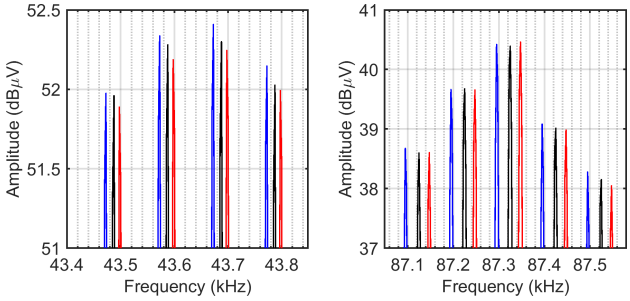

(a)

	Freq. (kHz)	Ampl. (dBuV)	Freq. (kHz)	Ampl. (dBuV)	Freq. (kHz)	Ampl. (dBuV)	Freq. (kHz)	Ampl. (dBuV)
49.90 Hz	43.67	52.41	43.57	52.34	43.77	52.15	43.47	51.98
50.00 Hz	43.69	52.30	43.59	52.28	43.79	52.03	43.49	51.96
50.01 Hz	43.70	52.24	43.60	52.19	43.80	51.99	43.50	51.89
49.90 Hz	87.30	40.42	87.19	39.66	87.39	39.08	87.09	38.67
50.00 Hz	87.33	40.39	87.22	39.68	87.42	39.02	87.13	38.60
50.01 Hz	87.35	40.46	87.25	39.66	87.45	38.99	87.15	38.60

(b)

Fig. 4: Detail of line spectra at different mains fundamental frequencies for LaCie P90: (a) snapshot of the two largest components with 50 Hz (black), 49.99 Hz (blue), 50.01 Hz (red); (b) amplitude values.

An interesting byproduct of a test under simulated mains frequency instability is that the frequency shift of spectrum components confirms their origin from the switching process following the zero crossings of the fundamental, whereas extraneous components from asynchronous sources will show a fix position not following the applied Δf.

B. Supply voltage amplitude

Three sets of tests have been performed with the supply voltage amplitude set at 210, 230 and 250 Vrms, thus almost covering the usual ±10% interval around the nominal value. Emissions of selected SMPS have been measured once temperature has stabilized for the P90 load condition: the obtained traces are shown in Figs. 5 and 6 and the most relevant components analyzed further in Tables I and II.

TABLE I: Amplitudes at selected frequencies for supply voltage variation (LaCie P90)

Supply voltage (V)	Peak frequency (kHz)				
	43.6	87.3	130.9	174.5	218.2
210	69.56	57.83	45.66	38.80	33.89
230	68.54	56.83	45.27	39.55	36.12
250	70.75	59.14	47.44	41.95	38.75

TABLE II: Amplitudes at selected frequencies for supply voltage variation (Shenzhen P90)

Supply voltage (V)	Peak frequency (kHz)				
	35.0	70.0	104.5	139.8	174.4
210	50.90	50.18	44.02	41.74	36.75
230	59.31	54.97	46.27	45.26	35.76
250	59.02	54.02	46.76	44.62	39.71

The dependency on the supply voltage level is not negligible: besides a non-monotonic dependency of 0.5 to 2 dB per 20 V change for LaCie P90, the Shenzhen was found with a different behavior showing low sensitivity from 230 V to

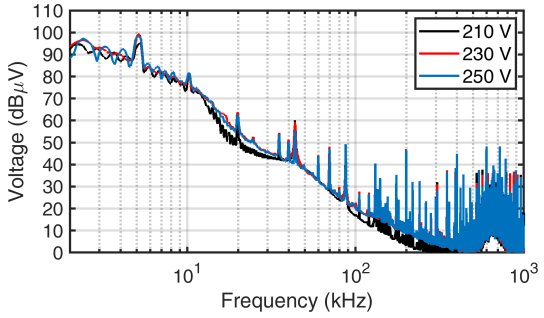

(a)

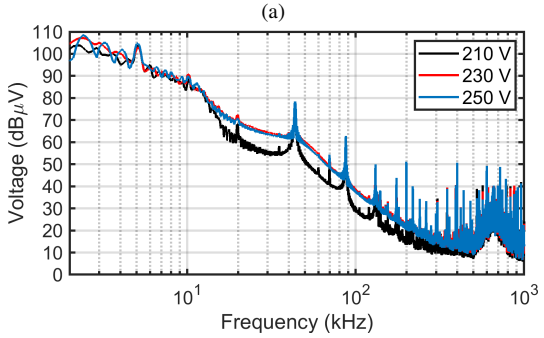

(b)

Fig. 5: Emissions vs. supply voltage amplitude (210 V, 230 V and 250 V): LaCie P90 (a) mean and (b) max hold profiles.

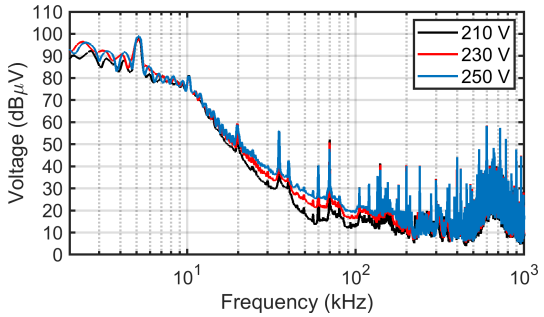

(a)

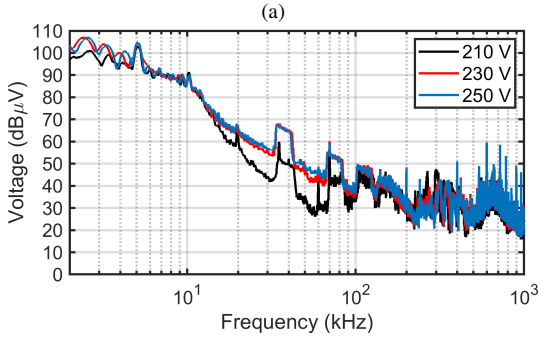

(b)

Fig. 6: Emissions vs. supply voltage amplitude (210 V, 230 V and 250 V): Shenzhen P90 (a) mean and (b) max hold profiles.

250 V, but a much different amplitude of components for the lowest value of 210 V.

C. Short-term variability

Short-term variations are evaluated with emissions recorded every 1 minute (see Fig. 7), where "st" quantities show:

- a good correspondence between the mean and median curves, indicating the absence of outliers;
- a compact distribution with indexes of dispersion below 0.5 for all supraharmonic emissions, lightly larger for RF emissions above 150 kHz;
- the random modulation SMPS (Shenzhen) is characterized by the presence of sporadic low emissions with $m_{st} > \mu_{st}$ and larger indexes of dispersion in the supraharmonic range;
- dispersion remains in a range of less than 4 dB that may be taken as the width of the confidence interval at k=1.

Interpreting instead "short term" as the time horizon limited to one record (here with 3 s duration), the values and considerations in Fig. 5 of [12] are confirmed with a dispersion that is one order of magnitude smaller than μ_{st} in Fig. 7.

D. EUT thermal transient and long-term variability

Thermal stabilization is the most relevant factor causing variability of emissions and affecting uncertainty. Repeated measurements of emissions during a thermal transient from no load to P90 starting from ambient temperature have been carried out. The tests have confirmed two points:

- thermal stabilization occurs with different dynamics for each SMPS, for which the equilibrium is reached after about 190 minutes for the LaCie and 130 minutes for the Shenzhen SMPS;
- variability between emission profiles during the thermal transient is significant until equilibrium is reached; this has been evaluated by means of long-term variability.

Results are reported in Figs. 9 and 10, with records separated by 10 minutes (from darker to lighter color for each group of traces): each trace corresponds to μ_{st} and m_{st}. Long-term variability affects in particular the characteristic components, because of changes in the internal mechanisms of emissions. The two SMPSs reached two slightly different operating temperatures starting from almost the same ambient temperature, set to about 21 °C in the laboratory during the winter season. The recorded temperatures during measured warm-up transients are reported in Fig. 8.

By inspecting the position of dark and light traces, two opposite behaviors emerge: a cold LaCie has lower emissions, whereas the Shenzhen starts with larger emissions. This poses the question of identifying the most representative conditions in an EMC perspective of worst-case emissions and, on the other hand, of operating under controlled conditions in a measurement perspective, so to improve reproducibility by reducing variability and systematic errors. Concerning the latter, carrying out tests when the final stable temperature is reached ensures minimal residual variation. Difference between first and last trace of each thermal transient profile is about 10 dB and is particularly evident up to about 150 kHz. It is briefly observed that the more compact traces of the median m, consistently smaller than the mean μ, indicate the presence of outliers with a significantly larger amplitude. This is confirmed by the observations in [16], where frequency scans with longer dwell time produce a significant number of unrelated peaks.

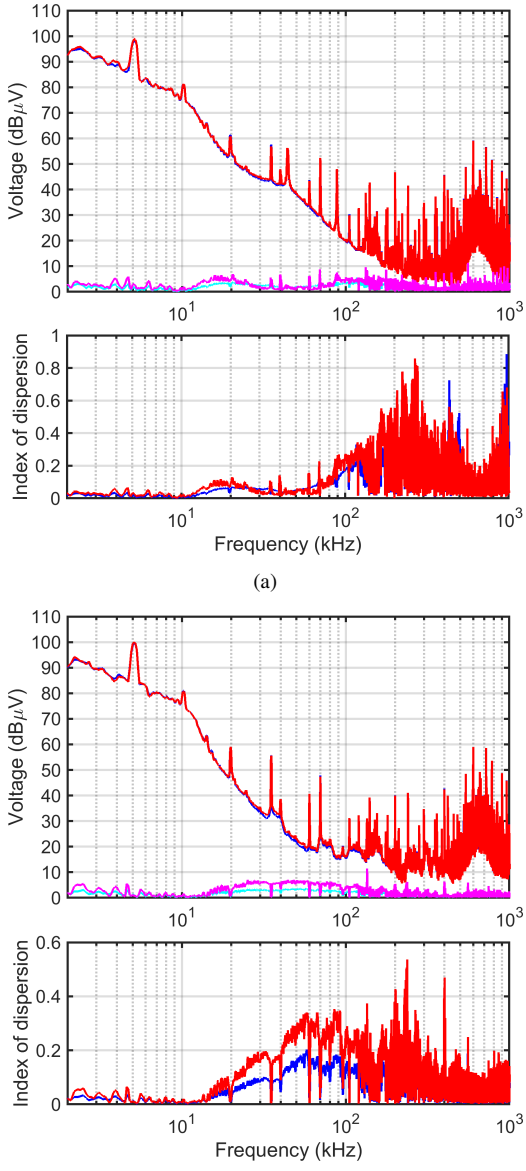

Fig. 7: Short-term variation of (a) LaCie P90 and (b) Shenzhen P90 using PXI time-domain 3-second records every minute, processed with RBW = 100 Hz and max hold: (top) μ_{st} and m_{st} (blue and red), standard deviation σ_{st} and inter-quartile range q_{st} (light blue and magenta); (bottom) indexes of dispersion as σ_{st}/μ_{st} (blue) and q_{st}/m_{st} (red).

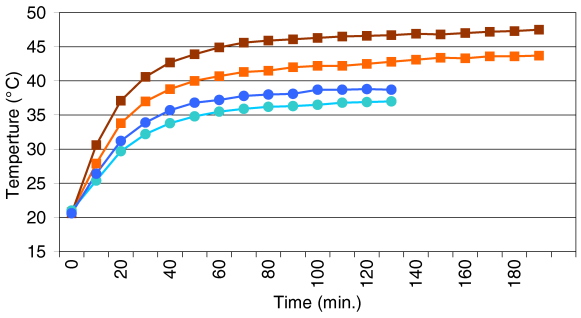

Fig. 8: Temperature values during warm-up transient in P90 conditions: LaCie (square, brown and orange for temperature taken on the top and bottom surface), Shenzhen (circle, blue and light blue for temperature taken on the top and bottom surface).

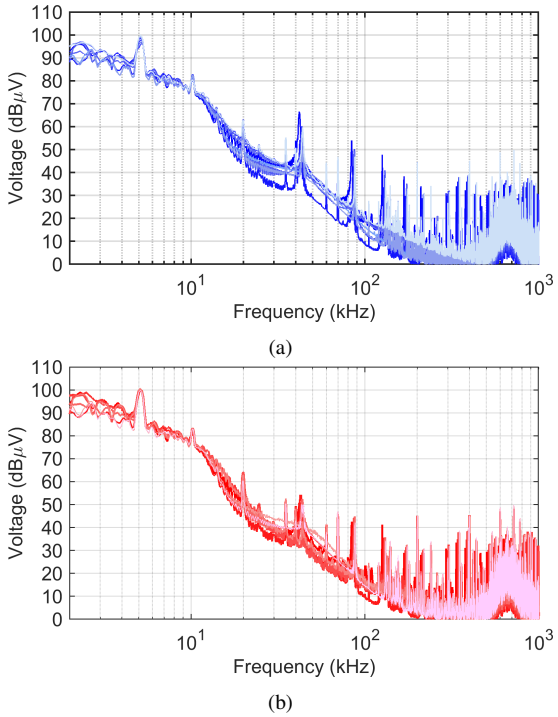

Fig. 9: Long-term variation of LaCie P90 frequency spectra calculated with STFT and Flat Top window, $T = 10\,\text{ms}$): (a) μ, (b) m.

V. Conclusion

Sources of uncertainty have been discussed for SMPS conducted emissions over the 2 to 1000 kHz range, thus including the supraharmonic interval. The tested SMPSs are two 12 VDC SMPS with nominal power of about 20 W and two different modulation methods. SMPS emissions are characterized by pulses and oscillations repeating synchronized to the mains voltage waveform.

Time- and frequency-domain measurements were carried out using a PXI board controlling also the EMI receiver. The setup includes a LISN, filtering stages before the PXI acquisition board and configurable resistive load for the DC output. Mains are provided by a controlled power supply.

Some elements affecting data dispersion and the uncertainty of conducted emission measurement have been demonstrated experimentally, showing that they should be disciplined by suitable procedures.

The influence of supply voltage amplitude is on average 0.5 dB per 10 V change, with a maximum of about 3 dB for the 210-250 V range. This is relevant to the overall measurement uncertainty and should be included as a test condition. Relevance is confirmed by the peculiar behavior of the characteristic components for the Shenzhen SMPS at 210 V.

The measured and calculated effects of the fundamental frequency instability indicate that the consequential variability is an order of magnitude smaller than that observed for the other phenomena (about 0.1 dB at most). However, it was noticed that the consequential shift of spectral components under a controlled mains frequency change may be a useful

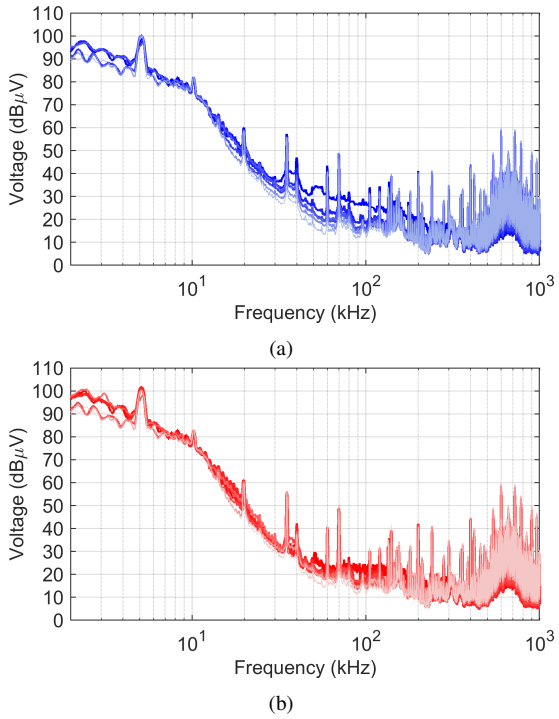

Fig. 10: Long-term variation of Shenzhen P90 frequency spectra calculated with STFT and Flat Top window, $T = 10\,\text{ms}$): (a) μ, (b) m.

method to identify extraneous disturbance components.

The short- and long-term variability of emissions was evaluated for two time horizons of 10 minutes and 2 hours, respectively. The observed short-term dispersion is limited to about 4 dB, indicating a relevant factor for quantification of uncertainty. Dispersion in the very short term (less than 1 second) was evaluated in [12] and found of the same order of the instrumental uncertainty. Long-term variability confirms quantitatively what was already known: the spread of traces is in the order of 10 dB, with much different behavior depending on the SMPS model. Measurements of emissions must be then carried out in stable thermal conditions that require a long time for thermal stabilization in the order of 2-3 hours. This does not mean that emissions measured during the thermal transient are not relevant, as probably an SMPS for information technology and similar equipment will operate almost always under thermal transient. However, from a measurement viewpoint, once thermal stabilization is reached, the resulting uncertainty is the short-term one and repeatability and reproducibility are improved.

The removal or control of the identified sources of systematic error and excessive variability would be a significant improvement of conducted emissions measurement of various power conversion equipment. This is particularly important for the increased number of such devices (exemplified as EV chargers, ITE power supplies, modern electrical appliances), for which compatibility levels and emission limits may be hard to define, especially with far-from-ideal conditions of data variability and measurement uncertainty.

REFERENCES

[1] IEC 61000-3-2, "Electromagnetic compatibility (emc) – Part 3-2: Limits – limits for harmonic current emissions (equipment input current $\leq$ 16 a per phase)," 2019.
[2] EN 55011, "Industrial, scientific and medical equipment —radio-frequency disturbance characteristics — limits and methods of measurement," 2021.
[3] EN 55032, "Electromagnetic compatibility of multimediaequipment — emission requirements," 2020.
[4] A. Mariscotti, "Power quality phenomena, standards, and proposed metrics for DC grids," *Energies*, vol. 14, no. 20, p. 6453, Oct. 2021.
[5] CISPR 14-1, "Electromagnetic compatibility - requirements for household appliances, electric tools and similar apparatus part 1: Emission," CISPR, 2016.
[6] CISPR 15, "Limits and methods of measurement of radio disturbance characteristics of electrical lighting and similar equipment," CISPR, 2018.
[7] EN 50065-1, "Signalling on low-voltage electrical installations in the frequency range 3 kHz to 148,5 kHz part 1: General requirements, frequency bands and electromagnetic disturbances," CENELEC, 2012.
[8] M. H. J. Bollen and S. K. Ronnberg, "Primary and secondary harmonics emission; harmonic interaction – a set of definitions," in *Proc. of Intern. Conf. on Harmonics and Quality of Power, ICHQP*, Belo Horizonte, Minas Gerais, Brazil, 2016, pp. 703 – 708. [Online]. Available: http://dx.doi.org/10.1109/ICHQP.2016.7783333
[9] IEC 61000-4-30, "Electromagnetic compatibility (EMC) – Part 4-30: Testing and measurement techniques – power quality measurement methods," IEC, 2015.
[10] IEC 61000-4-7, "Electromagnetic compatibility (EMC) – Part 4-7: Testing and measurement techniques – general guide on harmonics and interharmonics measurements and instrumentation, for power supply systems and equipment connected thereto," IEC, 2002.
[11] CISPR 16-1-1, "Specification for radio disturbance and immunity measuring apparatus and methods – part 1-1: Radio disturbance and immunity measuring apparatus – measuring apparatus," CISPR, 2019.
[12] A. Mariscotti and L. Sandrolini, "Variability of EMI measurement for switched mode power supplies EMI in the 2–1000 kHz range," in *2021 IEEE 11th International Workshop on Applied Measurements for Power Systems (AMPS)*. Cagliari, Italy: IEEE, Sep. 2021.
[13] L. Sandrolini and A. Mariscotti, "Impact of short-time fourier transform parameters on the accuracy of EMI spectra estimates in the 2-150 kHz supraharmonic interval," *Electric Power Systems Research*, vol. 195, p. 107130, Jun. 2021.
[14] J. B. Noshahr and B. M. Kalasar, "Evaluating emission and immunity of harmonics in the frequency range of 2–150 kHz caused by switching of static convertor in solar power plants," *CIRED - Open Access Proceedings Journal*, vol. 2017, no. 1, pp. 625–628, 2017.
[15] T. Yalcin, M. Ozdemir, P. Kostyla, and Z. Leonowicz, "Analysis of supra-harmonics in smart grids," in *Proc. 17th IEEE Intern. Conf. on Environment and Electrical Eng. and 1st IEEE Industrial and Commercial Power Systems Europe, EEEIC / I&CPS Europe 2017*, Milan, Italy, June 6-9 2017, pp. 1–4.
[16] L. Sandrolini and A. Mariscotti, "Waveform and spectral characteristics of supraharmonic unsymmetrical conducted EMI of switched-mode power supplies," *Electronics*, vol. 11, no. 4, p. 591, 2022.
[17] Agilent Technologies, "Ac power solutions — agilent models 6814b, 6834b, and 6843a," Tech. Rep. 5962-0887, 2000.
[18] CISPR 16-1-2, "Specification for radio disturbance and immunity measuring apparatus and methods – Part 1-2: Radio disturbance and immunity measuring apparatus – coupling devices for conducted disturbance measurements," CISPR, 2014.
[19] L. Wan, A. Khilnani, A. Hamid, F. Grassi, G. Spadacini, S. Pignari, M. Sumner, and D. Thomas, "Limitations in applying the existing LISN topologies for low frequency conducted emission measurements and possible solution," in *2021 Asia-Pacific International Symposium on Electromagnetic Compatibility (APEMC)*. IEEE, Sep. 2021.
[20] D. Istrate, D. Amaripadath, E. Toutain, R. Roche, and F. Gao, "Traceable measurements of harmonic (2 to 150) kHz emissions in smart grids: uncertainty calculation," *Journal of Sensors and Sensor Systems*, vol. 9, no. 2, pp. 375–381, Nov. 2020.
[21] Rohde and Schwarz, "ESRP EMI Receiver Specifications," 2017. [Online]. Available: https://scdn.rohde-schwarz.com/ur/pws/dl_downloads/dl_common_library/dl_brochures_and_datasheets/pdf_1/service_support_30/ESRP_dat-sw_en_3606-7576-22_v0400.pdf
[22] National Instruments, "PXIe-5164 specifications," Tech. Rep., 2019. [Online]. Available: https://www.ni.com/pdf/manuals/375320g.pdf

[23] Rohde and Schwarz, "ESH2-Z5 V-Network (4 lines 25 A)." [Online]. Available: https://www.rohde-schwarz.com/uk/product/esh2-z5-productstartpage_63493-9895.html

[24] A. Mariscotti, "Critical review of EMC standards for the measurement of radiated electromagnetic emissions from transit line and rolling stock," *Energies*, vol. 14, no. 3, p. 759, Feb. 2021.

[25] L. Alfieri, A. Bracale, G. Carpinelli, and A. Larsson, "Accurate assessment of waveform distortions up to 150 kHz due to fluorescent lamps," in *6th International Conference on Clean Electrical Power (ICCEP)*. Otranto, Italy: IEEE, Jun. 2017.

[26] S. K. Rönnberg, A. G. Castro, M. H. J. Bollen, A. Moreno-Munoz, and E. Romero-Cadaval, "Supraharmonics from power electronics converters," in *Proc. 9th International Conference on Compatibility and Power Electronics (CPE)*, Costa da Caparica, Portugal, June 24-26 2015, pp. 539–544.

[27] A. J. Collin, A. D. Femine, C. Landi, R. Langella, M. Luiso, and A. Testa, "The role of supply conditions on the measurement of high-frequency emissions," *IEEE Transactions on Instrumentation and Measurement*, vol. 69, no. 9, pp. 6667–6676, Sep. 2020.